
Masters Theses

Student Theses and Dissertations

Spring 2017

Cloth-air partitioning of oxybenzone

Jonathan T. Hill

Follow this and additional works at: https://scholarsmine.mst.edu/masters_theses

 Part of the [Environmental Engineering Commons](#), and the [Environmental Sciences Commons](#)

Department:

Recommended Citation

Hill, Jonathan T., "Cloth-air partitioning of oxybenzone" (2017). *Masters Theses*. 7648.
https://scholarsmine.mst.edu/masters_theses/7648

This thesis is brought to you by Scholars' Mine, a service of the Missouri S&T Library and Learning Resources. This work is protected by U. S. Copyright Law. Unauthorized use including reproduction for redistribution requires the permission of the copyright holder. For more information, please contact scholarsmine@mst.edu.

CLOTH-AIR PARTITIONING OF OXYBENZONE

BY

JONATHAN HILL

A THESIS

Presented to the Faculty of the Graduate School of the
MISSOURI UNIVERSITY OF SCIENCE AND TECHNOLOGY

In Partial Fulfillment of the Requirements for the Degree

MASTER OF SCIENCE IN ENVIRONMENTAL ENGINEERING

2017

Approved by

Glenn Morrison, Advisor
Mark Fitch
Fateme Rezaei

© 2017

Jonathan Hill

All Rights Reserved

ABSTRACT

Clothing has been proven to be a significant accumulator of chemicals from the air. Semi-volatile organic compounds (SVOCs) have a high affinity towards textiles, and measuring the equilibrium partition coefficient between cloth and air ($K_{\text{cloth-air}}$) for SVOCs is crucial in predicting human exposure to these compounds. This study aims to quantify $K_{\text{cloth-air}}$ for oxybenzone to contribute to a larger human exposure experiment carried out at the Technical University of Denmark (DTU). $K_{\text{cloth-air}}$ for oxybenzone was calculated using data collected from the exposure chamber at DTU and from performing extractions of oxybenzone in fabric samples from the experiment using HPLC. $K_{\text{cloth-air}}$ was calculated to be $5.9 \pm 2.1 \times 10^6$ ($\mu\text{g}/\text{m}^3$ per $\mu\text{g}/\text{m}^3$) for oxybenzone in cotton. Additionally, a lab scale measurement of this partition coefficient at 31 °C was also performed using headspace solid-phase microextraction (SPME). A comparison of the DTU fabric and a similar fabric using the headspace method resulted in $K_{\text{cloth-air}}$ values that ranged over an order of magnitude. The headspace SPME method for measuring $K_{\text{cloth-air}}$ seems promising, but improvements are necessary.

ACKNOWLEDGMENTS

I would first like to thank Dr. Glenn Morrison for providing me with the opportunity to conduct this research. I arrived at S&T without the slightest clue of what research I might be involved in. However, I became fascinated with indoor air quality, largely due to Dr. Morrison's enthusiasm and expertise. I could not have completed this project without his guidance and support.

Much credit is due to the members of Dr. Morrison's research group. Melissa Buechlein, Azin Eftekhari, and Arun Loka offered an immeasurable amount of training and expertise. Their willingness and eagerness to work together always made research very enjoyable.

Dr. Honglan Shi, Gary Abbot, and Ninu Madria were extremely helpful in resolving issues with the instruments in the lab. Their expertise extended beyond just maintenance, and their guidance was yet another source of valuable knowledge at S&T. I greatly appreciate Dr. Mark Fitch and Dr. Fateme Rezaei for accepting roles on my committee. I am also grateful to be an awardee of the Chancellor's Fellowship from the Department of Graduate Studies at S&T.

Lastly, I would like to thank several people who supported me in my personal life during my time at S&T. My parents raised me to be inquisitive and hardworking, which provided me a good platform for success - for this I will always be thankful. My two best friends, Archer and Leo, provided infinite joy while I was here. And I would most of all like to thank my wife, Brynn, for all of her love and support. Thank you.

TABLE OF CONTENTS

	Page
ABSTRACT	iii
ACKNOWLEDGMENTS	iv
LIST OF FIGURES	viii
LIST OF TABLES	ix
1. INTRODUCTION.....	1
1.1. PROPERTIES OF OXYBENZONE.....	2
1.2. SVOC EXPOSURE ROUTES.....	3
1.3. OXYBENZONE IN THE ENVIRONMENT.....	5
1.3.1. Oxybenzone in Water.....	5
1.3.2. Oxybenzone in the Air.....	6
1.4. OXYBENZONE TOXICOLOGY AND ECOLOGICAL EFFECTS	6
1.5. PARTITION COEFFICIENT.....	7
1.6. BP-3 EXPOSURE EXPERIMENTS	9
2. GOALS AND OBJECTIVES	11
2.1. OBJECTIVE 1	11
2.2. OBJECTIVE 2	11
2.3. OBJECTIVE 3	11
3. MATERIALS AND METHODS	12
3.1. MATERIALS.....	12
3.1.1. Oxybenzone.....	12
3.1.2. Thermal Desorption Tubes.....	12
3.1.3. SPME Polydimethylsiloxane Fibers.....	12
3.1.4. Fabrics.....	12
3.2. EXPERIMENTAL APPARATUS	13
3.2.1. Saturation Tube.....	13
3.2.2. Fabric Thickness Gauge.....	14
3.3. INSTRUMENTS.....	15
3.3.1. HPLC.....	15

3.3.2. FID-GC/FID.	15
3.3.3. GC-FID/SPME.	15
3.4. ANALYTICAL METHODS	15
3.4.1. Fabric Characteristics.	15
3.4.2. HPLC Method.	16
3.4.3. HPLC Calibration.	16
3.4.4. FID-GC/TD Method.	16
3.4.5. Unity Method.	17
3.4.6. Calibration of BP-3 using FID-GC/TD.	17
3.4.7. FID-GC/SPME Method.	17
3.4.8. Extraction Recovery Factor.	18
3.4.9. Calculation of BP-3 Concentration in DTU Samples.	19
3.4.10. Calculation of $K_{\text{cloth-air}}$ from DTU Samples.	21
3.4.11. Calculation of BP-3 Saturation Concentration and Vapor Pressure from Saturation Tube.	21
3.4.12. BP-3 Correction Factor from Saturation Tube for SPME.	23
3.4.13. Headspace Analysis.	24
4. RESULTS AND DISCUSSION	27
4.1. PARTITION COEFFICIENT FOR BP-3 FROM DTU EXPERIMENT	27
4.1.1. Fabric Analysis.	27
4.1.2. Extraction Recovery Factor.	27
4.1.3. BP-3 Concentration in Samples from DTU Experiment.	28
4.1.4. Partition Coefficient for BP-3 from DTU Experiment.	31
4.2. PARTITION COEFFICIENT USING SPME HEADSPACE ANALYSIS	32
4.2.1. Vapor Pressure of BP-3 Using Saturation Tube.	33
4.2.2. Correction Factor for SPME.	35
4.2.3. Partition Coefficient from SPME Headspace Analysis.	36
4.3. COMPARISON OF $K_{\text{CLOTH-AIR}}$ MEASUREMENTS.	39
5. CONCLUSIONS	42
5.1. OBJECTIVE 1.	42
5.1.1. Objective 1 Conclusion.	42

5.1.2. Objective 1 Suggestions for the Future.	42
5.2. OBJECTIVE 2.	42
5.2.1. Objective 2 Conclusions.....	43
5.2.2. Objective 2 Suggestions for the Future.	43
5.3. OBJECTIVE 3.	43
5.3.1. Objective 3 Conclusions.....	44
5.3.2. Objective 3 Suggestions for the Future.	44
REFERENCES.....	45
VITA	52

LIST OF FIGURES

	Page
Figure 3.1: Saturation Tube	14
Figure 3.2: Fabric Thickness Gauge	14
Figure 3.3: Fabric Sample Locations as seen from the inside of a DTU shirt sample.....	20
Figure 3.4: Temperature Control Box.....	25
Figure 3.5: Cross-sectional View of the Temperature Control Box	26
Figure 4.1: BP-3 Concentration in DTU Samples	30
Figure 4.2: $K_{\text{cloth-air}}$ from DTU Experiment.....	32
Figure 4.3: BP-3 Vapor Pressure vs. Temperature	34
Figure 4.4: Vapor Pressure vs. Temperature	35
Figure 4.5: Partition Coefficients from both methods	40

LIST OF TABLES

	Page
Table 1.1: Structure and Properties of Oxybenzone	2
Table 4.1: Recovery factor of BP-3 from cotton fabric for HPLC	28
Table 4.2: Oxybenzone Extraction from DTU samples using HPLC.....	29
Table 4.3: Cloth-Air Partition Coefficient of BP-3 at 25 °C	31
Table 4.4: Saturation Tube Results at Various Temperatures	33
Table 4.5: BP-3 SPME analysis at 31 °C (100% cotton denim fabric)	36
Table 4.6: BP-3 SPME analysis at 31 °C (100% cotton shirt)	38
Table 4.7: Headspace analysis of Sample 1 from DTU experiment (31 °C).....	39

1. INTRODUCTION

Semi-volatile organic compounds (SVOCs) can always be found in the indoor environment. Their commonly known sources include: construction materials, furniture, personal care products (PCPs), pesticides, flame retardants, and plasticizers [1-6]. One such SVOC, Benzophenone-3 (Oxybenzone, or BP-3), is found in a vast array of PCPs such as sunscreens, body lotions, hairspray, shampoo, and lipstick [7-12]. BP-3 is also commonly used as a light stabilizer in plastics and synthetic resins [13]. BP-3 has been linked to several adverse health and ecological effects including: allergic dermatitis, endocrine disruption, impacting the birthweight of infants, bioaccumulation in the marine environment, and coral bleaching [11]. BP-3 has been measured in the air of homes and cars at 3.27 and 10.7 ng/m³, respectively [14].

Because SVOCs are always present in the indoor environment, exposure to SVOCs is of significant concern. SVOCs will partition to every component of the indoor environment such as surfaces, air, particulate matter, and any other sorptive material [1, 2, 4, 6, 15-17]. Because of the ubiquity of SVOCs, exposure pathways include: inhalation, dermal uptake, and ingestion [1-6, 15, 17-19]. Efforts to model dermal uptake are underway, and human exposure experiments at Denmark Technical University are yielding interesting results [5, 20, 21].

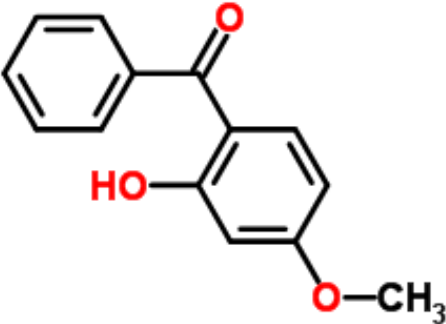
It has been hypothesized that clothing plays a significant role in the dermal uptake of SVOCs from the air [20]. To further understand the role of clothing, it is important to investigate the partitioning of SVOCs between fabric and air. The goal of this research is to determine the partition coefficient of BP-3 between cloth and air using two methods: extractions from the clothing worn during the DTU experiments, and a novel lab-scale

approach to quickly estimate partition coefficients using headspace solid-phase microextraction (SPME).

1.1. PROPERTIES OF OXYBENZONE

2-Hydroxy-4-methoxyphenyl-hpenylmethanone is also known as benzophenone-3, oxybenzone, and BP-3. The molecular formula of BP-3 is $C_{14}H_{12}O_3$. Table 1.1: Structure and Properties of Oxybenzone identifies some key properties of oxybenzone. [22]. BP-3 is in the class of ketones known as benzophenones, can be classified as an SVOC because of its low vapor pressure. BP-3 is a photostable UV absorber and is present in the formulation of the most efficacious sunscreens [23].

Table 1.1: Structure and Properties of Oxybenzone

Structure	Properties	
	MW (g/mol)	228.24
	Chemical Formula	$C_{14}H_{12}O_3$
	ρ (g/cm ³) at 20°C	1.2
	Melting Point (°C)	65
	Boiling Point (°C)	227
	Vapor Pressure (Pa) at 33 °C	2.71×10^{-3}
	Log K_{ow} (Log octanol-water partition coefficient at 25°C)	3.71

1.2. SVOC EXPOSURE ROUTES

The common SVOC exposure routes are: inhalation, ingestion, and dermal uptake. Inhalation is an important source of SVOC exposure. Exposure from inhalation is expressed in equation 1.2.

$$Exposure = C_g * InhR * ED \quad (1.2)$$

Where,

C_g - SVOC gas-phase concentration ($\mu\text{g}/\text{m}^3$)

$InhR$ - Inhalation rate (m^3/h)

ED - Duration of exposure (h).

This estimation of SVOC exposure from inhalation has been used to calculate daily doses of various SVOCs. Wensing et al. calculated the exposure to diethylhexyl phthalate (DEHP), di(n-butyl) phthalate, and tris(2-chloroethyl) phosphate (TCEP) to be 0.8, 3.91, and 3.18 $\mu\text{g}/(\text{kg}\cdot\text{d})$ [24]. The inhalation of particle-bound SVOCs has been shown to be a larger exposure route than inhalation from the gas-phase for some SVOCs [3, 15, 25]. Ingestion can occur after SVOCs have seeped into food sources [26].

Children are especially susceptible to ingesting SVOCs that are sorbed to surfaces and dust in the home because of their tendency to mouth objects [1, 24, 27, 28].

Many SVOCs, including: plasticizers, flame retardants, parabens, polychlorinated biphenyls (PCBs), polycyclic aromatic hydrocarbons (PAHs), and pesticides have been found in indoor dust [15, 25, 29, 30]. These SVOCs and their metabolites have also been detected in human blood and urine [31]. Initial efforts to model human exposure to SVOCs often only considered inhalation, ingestion, and dermal transfer as sources of

SVOC exposure [32-36]. A review on SVOC exposure by Weschler and Nazaroff in 2012 outlined the importance of SVOC exposure via dermal pathways [3]. A model was put forth to estimate dermal SVOC uptake from the air using an idealized mass transfer coefficient, the transdermal permeability coefficient [5]. The transdermal flux of a gas-phase SVOC can be calculated using equation 1.2.1.

$$J = C_g * k_{p_g} \quad (1.2.1)$$

Where,

J - Transdermal Flux ($\mu\text{g}/\text{m}^2\text{h}$)

k_{p_g} - Transdermal permeability coefficient (m/h)

This model was used to estimate SVOC exposure for common indoor air pollutants. Of the SVOCs with predicted k_{p_g} values, 33 were found to have dermal uptake-to-inhalation intake ratios of 1 or more. A study on the accumulation of gas-phase methamphetamine (meth) in skin oils showed that skin oil has the ability absorb meth from the air, further supporting the concept of dermal uptake from gas-phase SVOCs [18]. Weschler et al. later conducted a human exposure study to verify the dermal uptake of diethyl phthalate (DEP) and di(n-butyl) phthalate (DnBP). Dermal uptake, of DEP and DnBP as defined as absorption of gas-phase phthalates directly from air by skin was 4.0 and 3.1 $\mu\text{g}/(\mu\text{g}/\text{m}^3 \text{ in air})$, respectively [37]. Improvements on the dermal uptake model later included skin oil as a factor influencing the transdermal permeability coefficient [38]. A preliminary study on the dermal uptake of nicotine from air found that 368 to 413 μg of nicotine per m^2 of body area was absorbed directly from the air [39]. Wu et al.

estimated the dermal uptake of polybrominated diphenyl ethers (PBDEs) from E-waste burning to be as high as 0.65 and 1.1 ng/(kg*d) in adults and children, respectively [19].

The primary source of BP-3 exposure is from the application of sunscreens, which have formulations as high as 6% (w/w) in the U.S., and up to 10% (w/w) in Europe [40]. BP-3 is known to absorb through the skin, and its metabolites can be seen in urine. The systemic uptake of BP-3 after a whole-body application of 2 mg BP-3 per cm² body area was 1-2% [41]. BP-3 was found in 96.8% of 2517 urine samples in one study in the U.S., and was detected more frequently in females [10]. In another study BP-3 was detected in the amniotic fluid of 61% of pregnant women, and in 100% of the women's urine samples [9]. Schlumpf et al. reported the detection of BP-3 in 85.2% of human breastmilk samples, with a correlation between exposure and use of cosmetics [42]. They also suggested that human habits play the largest role in exposure to BP-3.

1.3. OXYBENZONE IN THE ENVIRONMENT

Oxybenzone has been found in numerous environmental media including: freshwater, seawater, wastewater influent, wastewater effluent, wastewater sludge, river sediment, in the air of residential and commercial buildings, and in human blood and urine [7, 10, 11, 14, 43-46].

1.3.1. Oxybenzone in Water. BP-3 has been widely recorded in aquatic environments around the world. BP-3 has been detected in surface water, wastewater and sewage sludge [7, 12, 43, 46-48], and aquatic life [7, 12, 43]. BP-3 concentrations in freshwater ranged from 2.5 to 175 ng/L, and the maximum concentration of BP-3 measured in seawater was 577 ng/L [8, 11]. BP-3 concentrations in wastewater influent and effluent were measured to be as high as 10,400 and 700 ng/L, respectively [7, 49].

1.3.2. Oxybenzone in the Air. Little research has been done on the occurrence of BP-3 in air. However, one study conducted by Wan et al. collected 81 samples of indoor air and found BP-3 in all 81 samples [14]. The mean BP-3 concentrations ranged from 0.47 ng/m³ in laboratories to 10.7 ng/m³ in cars. They also identified the median ratio of concentrations between the vapor phase and bulk air to be 0.4, which suggests that BP-3 is mostly found in the particulate phase in indoor air. They calculated an estimated daily intake from inhalation of up to 41.1 and 134 ng/day for adults in homes and cars, respectively.

1.4. OXYBENZONE TOXICOLOGY AND ECOLOGICAL EFFECTS

In the first study of its kind, Schlumpf et al. demonstrated the estrogenicity of BP-3 [50]. *In vitro* assays of MCF-7 breast cancer cells exposed to BP-3 showed a dose-dependent increase in cell proliferation. The excretion of the estrogen-regulated pS2 protein also showed a dose-dependent increase in response to BP-3. Additionally, *in vivo* immature rat uterotrophic assays in Long-Evans rats showed a dose-dependent increase in uterine weight in response to BP-3 exposure. Attempts to verify these results were inconclusive, but suggested that the endocrine disrupting effect of BP-3 was perhaps not expressed by typical estrogenic markers [51]. BP-3 has demonstrated an agonistic effect on thyroidal activity [52]. In an *in vivo* study in mice, BP-3 caused a decrease in sperm density and changes in the estrous cycle [53]. BP-3 was shown to alter the genes of zebrafish involved in hormonal pathways and alter the phenotypic sex ratio in zebrafish, decreasing the amount of males born after exposure [54, 55]. BP-3 has also been linked to coral bleaching [56, 57]. Donavaro et al. first connected coral bleaching with BP-3 exposure and identified that BP-3 promoted viral infections of coral [56]. Downs et al.

tested the effects of BP-3 on sea coral, and discovered that current BP-3 concentrations in some seawater samples exceeded the effect concentration (EC_{20} , 6.5 to 10 $\mu\text{g/L}$) and the lethal concentration (LC_{50} , 139 to 779 $\mu\text{g/L}$) for 24 hour exposures [57]. They suggested that sunscreen use at recreational beaches was of major concern for the health of coral reefs and the threat of BP-3 extends much further than the immediate swimming area [57].

1.5. PARTITION COEFFICIENT

A partition coefficient is the distribution of a solute in two immiscible phases at equilibrium [58]. One of the simplest theoretical approaches to describe a partition coefficient is to use an extension of Henry's law, in which a gas is in equilibrium with its solution in a solvent. Because the concentration of a compound in the gaseous phase is proportional to its partial pressure, Henry's law can take the form of Equation 1.5.

$$\frac{C_2}{C_1} \approx K \quad (1.5)$$

Where,

C_1 - Partial pressure of solute in gaseous phase (atm)

C_2 - Concentration of solute in solution (mol L^{-1})

K - Henry's constant (L atm mol^{-1})

Partition coefficients have various units and applications. A widely used partition coefficient in pharmacology and environmental research is the octanol-water partition coefficient (K_{o-w}). This partition coefficient describes the ratio of solute concentrations in octanol and water, and is used as an indicator for hydrophobicity. Chemical species with high octanol-water partition coefficients are hydrophobic, preferring the non-water phase,

and those with low octanol-water partition coefficients prefer the water phase . Hydrophobic compounds are often lipophilic and biologically accumulate in the environment. The air-water partition (K_{a-w}) coefficient for compounds of environmental concern is another frequently used partition coefficient [59]. A compound's K_{a-w} is essential to determining its fate in the environment. For example, sulfur dioxide has a large K_{a-w} and will partition from air to water (acid rain), while benzene has a small K_{a-w} and will partition from the aqueous phase to air [60]. Other partition coefficients important to environmental studies include: gas-dust partitioning of SVOCs, soil-water partitioning of pharmaceuticals and other compounds, and cloth-air partitioning of SVOCs [18, 20, 27, 61-63].

The partitioning of compounds between fabrics and air has been referred to as gas-fabric and cloth-air partitioning (hereafter cloth-air). This partition coefficient is defined by equation 1.5.1.

$$K_{cloth-air} = \frac{C_{cloth}}{C_{air}} \quad (1.5.1)$$

Where,

C_{cloth} - Concentration of compound in cloth ($\mu\text{g}/\text{m}^3$)

C^{air} - Concentration of compound in air ($\mu\text{g}/\text{m}^3$)

$K_{cloth-air}$ - Cloth-air partition coefficient (dimensionless)

The cloth-air partition coefficients between several fabrics and compounds have been reported. As shown in 1.5.1, the partition coefficient is normalized by the cloth volume; it has also been defined as normalized by area or mass. Saini et al. measured the area-normalized cloth-air partition coefficient for several PBDEs, with partition

coefficients ranging from 1.3×10^4 to 2.2×10^4 ($\text{pg m}^2/\text{pg m}^3$) for cotton and 1.6×10^4 to 6.4×10^4 for polyester at 25 °C [64]. They demonstrated that $k_{\text{cloth-air}}$ decreases as temperature increases for SVOCs because an increase in vapor pressure results in more of the SVOC in the gas-phase. They also determined that non-polar SVOCs partition more to non-polar textiles and polar SVOCs partition more to hygroscopic textiles, as demonstrated with non-polar PBDEs having higher partition coefficients with polyester fabrics [61, 64]. Morrison et al. measured partition coefficients for phthalates in clothing, finding the mean $k_{\text{cloth-air}}$ of 2.6×10^5 for DEP and 3.9×10^6 for DnBP [27]. Morrison et al. also measured $k_{\text{cloth-air}}$ for meth to be 1.22×10^4 for polyester and 4.72×10^5 for cotton at 30% R.H., and 1.13×10^4 for polyester and 8.84×10^5 for a cotton/polyester blend at 60% R.H. [18]. These results show that as relative humidity increases, the partitioning of polar SVOCs to hygroscopic fabrics increases.

1.6. BP-3 EXPOSURE EXPERIMENTS

Morrison et al. hypothesized that dermal uptake from clothing contaminated with BP-3 is a significant contributor to the overall body burden of BP-3 [21]. Recently, human exposure experiments were carried out at Denmark Technical University (DTU) to test this hypothesis (Morrison et al., manuscript in preparation). A small chamber was prepared to expose shirts to airborne BP-3. BP-3 was melted and brushed onto three 0.15 m² aluminum pans. The pans were placed in the bottom of the chamber and a computer fan was installed to facilitate air mixing. A final airborne concentration of 4.4 ng/L in the chamber was achieved. Four long-sleeved 100% cotton t-shirts were hung in the chamber and left to equilibrate at room temperature for 32 days at 25 °C. At the time of this experiment, it was unknown if the shirts had reached equilibrium in the exposure

chamber. Three of the shirts were worn by participants in the exposure study and one was unworn. After the exposure experiment, the shirts were shipped to Missouri University of Science and Technology for analysis. They concluded that dermal uptake from clothing equilibrated with BP-3-laden air could be greater than dermal uptake on bare skin under the same conditions. An accurate measurement of the partition coefficient of BP-3 in cloth and air would help model the overall phenomena of dermal uptake from clothing, and is the motivation for the research presented in this thesis. Because of the quasi-equilibrium state of the shirts in the dosing chamber, only an effective partition coefficient can be calculated using the materials and information from the DTU experiment.

2. GOALS AND OBJECTIVES

2.1. OBJECTIVE 1

Quantify the concentration of BP-3 in the fabric from the DTU experiments.

2.2. OBJECTIVE 2

Calculate the effective partition coefficient of BP-3 between cloth and air based on the assumption of quasi-equilibrium conditions from the DTU experiments.

2.3. OBJECTIVE 3

Measure the partition coefficient at 31 °C between cloth and air for oxybenzone using a novel lab-scale approach with headspace solid-phase microextraction.

3. MATERIALS AND METHODS

The following materials and methods were used to quantify the partition coefficient of BP-3 in cloth and air to meet the objectives of this project.

3.1. MATERIALS

Oxybenzone, thermal desorption tubes, PDMS-SPME fibers, and various fabrics were used to complete this project.

3.1.1. Oxybenzone. 98% Benzophenone-3 (oxybenzone, or BP-3) was purchased from Sigma Aldrich, catalog number H36206. The BP-3 was used to determine the percent recovery during extraction from cloth, for determining the vapor pressure of BP-3, and for fabric spiking during SPME analysis.

3.1.2. Thermal Desorption Tubes. Thermal desorption tubes filled with 300 mg Tenax TA from Markes International were used to measure the air concentration of BP-3.

3.1.3. SPME Polydimethylsiloxane Fibers. SPME Polydimethylsiloxane (PDMS) fiber assemblies, size 23ga, with a fused 7 μ m thick PDMS coating were purchased from Sigma Aldrich, catalog number 57291-U. The fibers were used for the headspace SPME analysis of fabrics spiked with BP-3.

3.1.4. Fabrics. Several types of fabric were used in this study. Long-sleeve blue t-shirts made of 100% cotton were purchased in Lyngby, Denmark, for the human exposure experiments. Long-sleeve green t-shirts made of 100% cotton were purchased from the S&T Store in Rolla, Missouri, and 100% cotton Wrangler blue jeans were purchased at a local retailer in Rolla, Missouri.

3.2. EXPERIMENTAL APPARATUS

Several apparatuses were designed and built to accomplish the goals set forth in this research, including: a saturation tube, a fabric thickness gauge, and small temperature control chambers.

3.2.1. Saturation Tube. A saturation tube was made to employ the gas saturation method for determining the vapor pressure of BP-3 at various temperatures [65]. The saturation tube was made from Teflon® tubing with dimensions of 2 m x 4 mm. The tube was filled with 666 glass beads of 3 mm diameter and fitted with Swagelok fittings on each end. The tube was filled with 12 mL of a solution of 400 µg BP-3 in Acetonitrile. The tube was held in a “U” shape and both ends were opened. The tube was then slowly purged with ultra-high purity nitrogen to allow the solvent to evaporate. This procedure resulted in the glass beads being entirely coated with solid BP-3. Glass wool was inserted into each end of the tube, occupying approximately 1 cm of tubing. Two thermal desorption tubes were placed in series at one end of the tube. The first desorption tube functioned as the primary sampling tube, and the second desorption tube functioned as a “breakthrough” tube. Further tubing connected the sorption tubes to a mass flow controller and pump. Figure 3.1: Saturation Tube is an illustration of the saturation tube. The tube was thermostated in a temperature controlled chamber. The tube was allowed to stand at each desired temperature for 24 hours before sampling, and air was pumped through the tube for one hour before sampling on sorption tubes began.

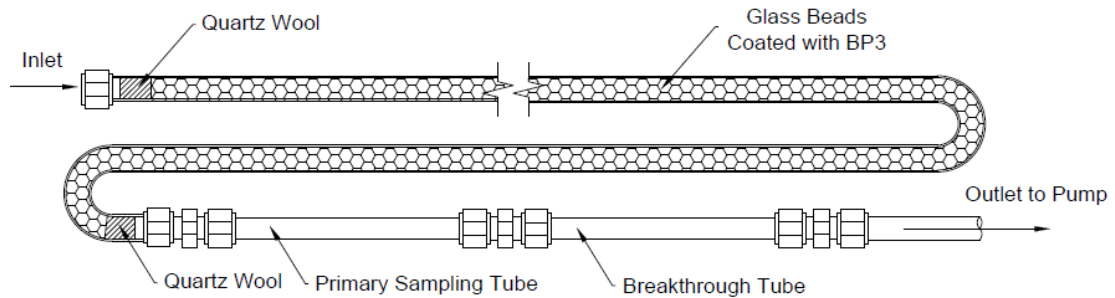


Figure 3.1: Saturation Tube

3.2.2. Fabric Thickness Gauge. A fabric thickness gauge was designed to meet ASTM standard D1777-96 for textile thickness measurements [66]. An analog thickness gauge was outfitted with a circular anvil of 38 mm diameter and a circular presser foot of 28.7 mm. A cylinder of aluminum weighing 272 g was added to the top of the contact rod to apply a force of 0.6 psi to the fabric during measurement. The thickness gauge is shown in figure 3.2: Fabric Thickness Gauge.



Figure 3.2: Fabric Thickness Gauge

3.3. INSTRUMENTS

Several different types of gas chromatographs were used to help accomplish the goals set forth in this study.

3.3.1. HPLC. High Pressure Liquid Chromatography (HPLC), performed with a LabTech UV600 series detector, pumps, and autosampler, was used for the analysis of BP-3 extracted in acetonitrile from clothing.

3.3.2. FID-GC/FID. An Agilent model 6890 series Gas Chromatograph with a Flame Ionization Detector (FID-GC) was used to analyze BP-3 on sorption tubes. A Markes International UNITY Thermal Desorber with an Ultra TD auto sampler facilitated desorption of BP-3 from the sorption tubes to the FID-GC for analysis.

3.3.3. GC-FID/SPME. An Agilent model 7890A series FID-GC was used to analyze BP-3 in headspace air. The GC was equipped with a CTC Analytics CombiPal Autosampler system.

3.4. ANALYTICAL METHODS

The follow methods of analysis were employed to achieve the goals set forth in this study.

3.4.1. Fabric Characteristics. The thickness of the fabric was measured in order to determine its density. Four samples of fabric were cut to at least 20% greater than the size of the presser foot of the fabric thickness gauge. The sample thicknesses were measured and recorded. Next, five square samples of varying dimensions (9, 18, 25, 38, and 100 cm²) were carefully cut out and weighed. The area of the cloth was multiplied by the average thickness of the material to determine the volume of the cloth sample. The

volume of the cloth sample was divided by the weight of the cloth sample to determine the density. The average density was determined to be $0.282 \text{ g/cm}^3 \pm 0.01$.

3.4.2. HPLC Method. A Synergi™ 4 μm Hydro-RP 80 Å, LC column (250 mm x 4.6 mm) was purchased from Phenomenex. The autosampler mode was 30 μL partial loop injection. The isocratic mode used 10% water and 90% acetonitrile with a constant flow of 1 mL/min. A wash of 500 μL of 50% water and 50% acetonitrile was done after each sample. BP-3 was detected at 325 nm. This method was adapted from a similar methods used for the detection of BP-3 using HPLC [67, 68].

3.4.3. HPLC Calibration. The HPLC was calibrated by analyzing various concentrations of a solution of BP-3 in acetonitrile. A solution of 100 $\mu\text{g/mL}$ BP-3 in acetonitrile was prepared. Six dilutions of this solution were also prepared to make 2, 7, 10, 15, 25, and 50 $\mu\text{g/mL}$ concentrations. Two samples of each concentration were analyzed using the method developed for BP-3. The resulting calibration curve had an R^2 value of 0.999. The limit of detection was $<0.1 \mu\text{g/mL}$.

3.4.4. FID-GC/TD Method. The FID-GC was equipped with a HP-5 5% Phenyl Methyl Siloxane (30 m x 320 μm x 0.25 μm) capillary column. The oven temperature was programmed to start at 40 °C for 2 min, then ramped up 40 °C/min to 250 °C for 4 min, then ramped up 50 °C/min to 300 °C for 4 min. The inlet temperature was set to 260 °C with a pressure of 8 psi for a total flow of 4.5 mL/min (splitless). Helium was used as the carrier gas at a flow of 4.5 mL/min, and nitrogen was used as the makeup gas at a flow of 43.7 mL/min. The detector temperature was 300 °C with a hydrogen flow of 40 mL/min and air flow of 450 mL/min. The retention time of BP-3 was approximately 9.8

minutes. This method was adapted from an analytical method used for the analysis of phthalates [69].

3.4.5. Unity Method. The primary desorption temperature was 290 °C for 15 min with a flow rate of 20 mL/min (splitless). The secondary desorption packing material was unsilanized glass wool with a temperature of 300 °C for 3 min and a split flow of 5 mL/min. The transfer line temperature was 185 °C. Samples were injected three times. The responses from the first two injections were added to show the total response. The third injection was to ensure that the entire mass of BP-3 was desorbed during the first two injections.

3.4.6. Calibration of BP-3 using FID-GC/TD. The FID-GC/TD was calibrated by spiking known masses of BP-3 to sorption tubes packed with Tenax TA. A stock solution of 1,000 µg/mL BP-3 in 1% methanol in pentane was prepared. Two dilutions were made from the stock solution to make 100 µg/mL and 250 µg/mL of BP-3 in 1% methanol in pentane. A total of seven masses were used to make the calibration curve (0, 100, 200, 250, 300, 400, and 500 ng). The various masses of BP-3 were achieved by adding a known volume of the dilutions to a thermal desorption tube (i.e. 200 ng of BP-3 was applied by injecting 2 µL of the 100 µg/mL solution). The calibration curve had an R^2 value of 0.98.

3.4.7. FID-GC/SPME Method. The FID-GC was equipped with a HP-5 5% Phenyl Methyl Siloxane (30 m x 320 µm x 0.25 µm) capillary column. The SPME fiber desorption time is 14 minutes. The oven temperature was programmed to start at 40 °C for 1 min, then 15 °C/min to 180 °C for 3 min, then 5 °C/min to 220 °C for 5 min. The inlet heater was set to 280 °C with a pressure of 6 psi and a total flow of 54.3 mL/min

(splitless). The FID detector temperature was 300 °C with a H₂ flow of 40 mL/min and an air flow of 450 mL/min.

3.4.8. Extraction Recovery Factor. An experiment was performed to determine the percent recovery during extractions of BP-3 from fabric. Seven fabric samples of approximately 2 cm x 4 cm were cut from a cotton t-shirt. A solution of 100 µg/mL BP-3 in acetonitrile was prepared. Three fabric samples were spiked with 250 µL of the solution, and three samples were spiked with 500 µL of the solution. One sample was spiked with 500 µL of pure acetonitrile to serve as a blank. The fabric samples were left in a fume hood at ambient temperature for 30 minutes to allow the acetonitrile to evaporate. Each fabric sample was then placed in a 12-mL glass vial with clean forceps. The vials were filled with 5 mL of acetonitrile, capped, and sonicated in a Branson model 2210 series sonicator for 30 minutes. Acetonitrile was chosen as an extraction solvent because its common use as a polar solvent makes it compatible for the moderately polar BP-3. The samples were removed from the sonicator and allowed to return to room temperature. Approximately 1.5 mL of the solution in the vials was withdrawn using 2-mL syringes with 0.2-µm nylon filters and transferred to 2-mL HPLC vials. The recovery factor was calculated using equation (3.4.8).

$$R = \frac{m_{BP3,HPLC}}{m_{BP3}} * 100\% \quad (3.4.8)$$

Where,

R - Extraction recovery factor (%)

$m_{BP-3,HPLC}$ - Mass of BP-3 detected by HPLC (µg)

m_{BP-3} -Mass of BP-3 spiked onto clothing before extraction (µg)

3.4.9. Calculation of BP-3 Concentration in DTU Samples. The concentrations of BP-3 in the clothing samples from the DTU experiment were determined using HPLC. The samples were transported in sealed glass jars to Missouri University of Science and Technology via international mail. The backs of the shirts from DTU were opened from their transport containers and laid on clean sheets of aluminum foil. Four samples of approximately the same size were cut from the upper left, upper right, lower left, and lower right sections of the shirt as shown in Figure 3.3: Fabric Sample Locations as seen from the inside of a DTU shirt sample. These samples were weighed and an estimation of each sample volume was made using the previously measured fabric characteristics. The samples were then placed in 12-mL glass vials. Each vial was filled with 5 mL of acetonitrile, capped, and sonicated for 30 minutes. The samples were removed from the sonicator and allowed to return to room temperature. Approximately 1.5 mL of the solution in the vials was withdrawn using 2-mL syringes with 0.2- μ m nylon filters and transferred to 2-mL HPLC vials. These samples were analyzed and quantified using the previously mentioned calibration and extraction recovery percentage.

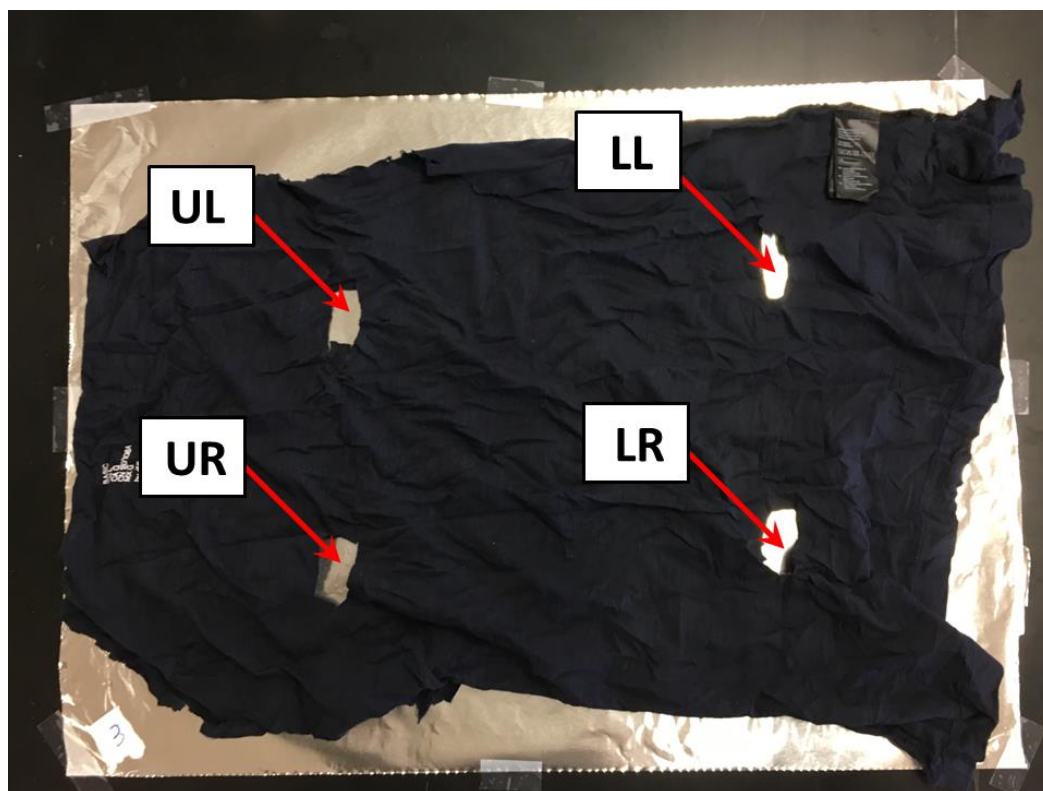


Figure 3.3: Fabric Sample Locations as seen from the inside of a DTU shirt sample

The concentration of BP-3 in the clothing samples was calculated using equation (3.4.9).

$$C_{BP3,cloth} = \frac{V * C_{BP3,ext}}{v * R} \quad (3.4.9)$$

Where,

$C_{BP-3,ext}$ - Concentration of BP-3 in the extraction solution ($\mu\text{g/mL}$)

V - Volume of extraction solution (5 mL)

v - Volume of fabric sample (m^3)

R - Recovery factor

3.4.10. Calculation of $K_{cloth-air}$ from DTU Samples. The concentration of BP-3 in the cloth samples and the air concentration of BP-3 from the DTU experiments were used to calculate the cloth-air partition coefficient of BP-3 ($K_{cloth-air}$). Air samples were collected and analyzed for BP-3 by the Fraunhofer Institute (WKI) in Braunschweig Germany. The average air concentration, $4.4 \mu\text{g}/\text{m}^3$, reported by WKI is used in this analysis. The average BP-3 concentration in the cloth was divided by the average air concentration of BP-3 in the experimental chamber. $K_{cloth-air}$ was calculated using equation (3.4.10).

$$K_{cloth-air} = \frac{C_{BP3,cloth}}{C_{BP3,air}} \quad (3.4.10)$$

Where,

$C_{BP-3, cloth}$ - Concentration of BP-3 in the cloth ($\mu\text{g}/\text{m}^3$)

$C_{BP-3, air}$ - Concentration of BP-3 in the air ($\mu\text{g}/\text{m}^3$)

3.4.11. Calculation of BP-3 Saturation Concentration and Vapor Pressure from Saturation Tube. The saturation concentration and vapor pressure of BP-3 was determined using the previously described saturation tube in a temperature controlled chamber. The saturation concentration measurements were conducted at 25, 27, 31, and 35 °C. The saturation tube was allowed to stand for a minimum of 24 hours after each temperature change before sampling. The gas-phase concentration of BP-3 was determined by drawing 20 mL/min of air through the saturation tube assembly. Samples and duplicates were taken for 1 hour, for a sample volume of 1.2 L. The sorption tubes

were then analyzed on the FID-GC/TD to determine the mass of BP-3 on the sorption tube. The saturation concentration was calculated using equation 3.4.11.1.

$$C_s = \frac{w}{Q * t} \quad (3.4.11.1)$$

Where,

C_s - Saturation concentration of BP-3 ($\mu\text{g}/\text{m}^3$)

w - Mass of BP-3 on sorption tube (μg)

Q - Flow of air through the saturation tube (m^3/min)

t - Sampling time (min)

The vapor pressure of BP-3 was also calculated using the ideal gas law as expressed in equation (3.4.11.2).

$$P_v = \frac{w}{Q t} * \frac{RT}{M} \quad (3.4.11.2)$$

Where,

P_v - Vapor pressure of BP-3 (kPa)

w - Mass of BP-3 on sorption tube (g)

Q - Flow rate of air through the saturation tube (cm^3/min)

R - Gas constant ($8.314 \text{ cm}^3 \text{ kPa K}^{-1} \text{ mol}^{-1}$)

T - Temperature (K)

M - Molar mass of BP-3 (228.24 g/mol)

3.4.12. BP-3 Correction Factor from Saturation Tube for SPME. The vapor pressure of BP-3 was needed to calibrate the FID-GC/SPME for analysis. After establishing the concentration of BP-3 in air at saturation, the FID-GC/SPME response for this saturated air was targeted. A 20-mL glass headspace vial was filled with approximately 0.5 g of pure BP-3 and capped. The sealed vial was then placed in an incubator oven at 70 °C to melt the crystals. After the BP-3 melted, the vial was turned upside down and slowly rotated so that the liquid BP-3 would evenly coat the walls of the vial. Once the walls were evenly coated, the vial was left at room temperature for the liquid to solidify. The vial was allowed at least 24 hours to equilibrate at various temperatures before headspace extractions with the SPME fiber. The time of extraction was 14 minutes. The response on the FID-GC/SPME chromatogram for each temperature at saturation relates to the vapor pressure of BP-3 at that temperature. The calibration was determined to be the peak area of the BP-3 response on the chromatogram divided by the BP-3 gas-phase concentration for that temperature. The concentration of BP-3 in the headspace air was calculated using the correction factor expressed in equation (3.4.12).

$$X = C_s/PA \quad (3.4.12)$$

Where,

X - The correction factor

C_s - Saturated concentration (µg/m³)

PA - Peak area from chromatogram integration

The concentration of BP-3 in the headspace air from a SPME analysis is equal to the peak area of the BP-3 peak in the chromatogram multiplied by the correction factor.

3.4.13. Headspace Analysis. The headspace concentration of BP-3 using SPME was determined by spiking fabric samples with a known mass of BP-3, placing the sample in a headspace vial, and measuring the concentration of BP-3 in the air of a vial. Fabric samples were cut to 4 cm x 4 cm squares, and each sample was weighed. Solutions of 25, 50, and 100 $\mu\text{g/mL}$ BP-3 in acetonitrile were prepared. Fabric samples were placed on a Teflon sheet and 1 mL of solution was spiked to impregnate the fabric with BP-3. The samples were placed in a fume hood for 30 minutes to allow the acetonitrile to evaporate. The dry fabric samples were then placed in 20-mL headspace vials with clean forceps. These samples were given 24 hours for the BP-3 to equilibrate with the cloth and air. The samples were held at a constant temperature in an augmented Peak brand 12-volt cooler/warmer box, and the temperature was maintained at ± 1 $^{\circ}\text{C}$. The box was outfitted with sampling ports to ensure the temperature was not affected by the sampling procedure. Figure 3.4: Temperature Control Box shows the exterior of the temperature control box, and Figure 3.5: Cross-sectional View of Temperature Control Box shows a cross-sectional view of the inside of the box. Not shown in Figure 3.5. is the small computer fan and the thermocouple. The vials were sampled from with the PDMS SPME fiber for 14 minutes, and then analyzed on the FID-GC/SPME instrument. $K_{\text{cloth-air}}$ was calculated using equation 3.4.10.



Figure 3.4: Temperature Control Box

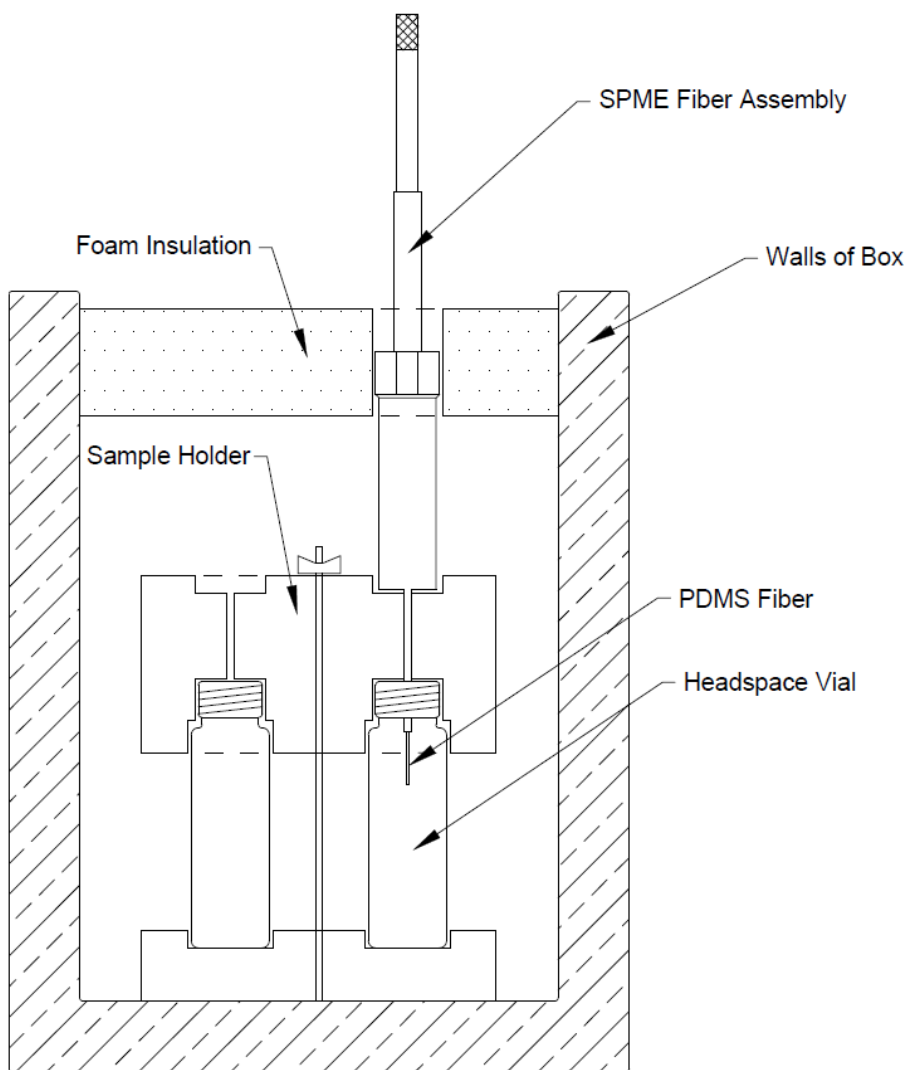


Figure 3.5: Cross-sectional View of the Temperature Control Box

4. RESULTS AND DISCUSSION

The results of this study demonstrate that the partition coefficient of a BP-3 in cloth and air can be calculated from clothing samples that have equilibrated with BP-3 in the air of an experimental chamber. The partition coefficient was also estimated using SPME headspace analysis, but method improvements are necessary in order to verify $K_{\text{cloth-air}}$ for the DTU samples.

4.1. PARTITION COEFFICIENT FOR BP-3 FROM DTU EXPERIMENT

The partition coefficient of BP-3 in cloth and air from the DTU samples was calculated. The fabric thickness was measured to calculate the density using the mass of a known area of fabric. The concentration of BP-3 in the fabric samples from DTU was determined using solvent extraction and HPLC. The concentration of BP-3 in the fabric was compared to the air concentration of BP-3 in the DTU experimental chamber to determine $K_{\text{cloth-air}}$.

4.1.1. Fabric Analysis. The fabric thickness of the DTU shirts measured using the thickness gauge described in 3.2.2. and 3.4.1. was determined to be $0.0622 \text{ cm} \pm 0.01$. Using this thickness and a known area of cloth, the density was measured to be $0.282 \text{ g/cm}^3 \pm 0.01$. The density of the fabric measured at this stage of the experiment was later used to quantify the volume of an irregular fabric sample with a known mass. The thickness of the jean material used for the first headspace analysis was $0.138 \text{ cm} \pm 0.01$.

4.1.2. Extraction Recovery Factor The recovery factor of the extraction procedure described in 3.4.8. was determined to be $90.2\% \pm 1.9$. The results of the recovery experiment are shown in Table 4.1: Recovery factor of BP-3 from cotton fabric for HPLC.

Table 4.1: Recovery factor of BP-3 from cotton fabric for HPLC

Mass Spiked (μg)	Mass detected (μg)	Recovery
0	0	n/a
25	22.07	0.88
25	22.04	0.88
25	23.69	0.95
25	22.01	0.88
25	21.85	0.87
25	21.82	0.87
50	46.96	0.94
50	46.86	0.94
Mean		90.2%
St. Dev.		3%

This recovery factor of 90.2% is similar to other extraction recoveries achieved in studies extracting synthetic dyes and water repellants from textiles, which range from 82% to 106% [70-72].

4.1.3. BP-3 Concentration in Samples from DTU Experiment. The concentration of BP-3 in the shirts from the DTU experiment was measured using the analytical method described in 3.4.9. The results are shown in Table 4.2: Oxybenzone Extraction from DTU samples using HPLC.

Table 4.2: Oxybenzone Extraction from DTU samples using HPLC

*Denotes sample location, i.e. UL = upper left of shirt back, LR = lower right of shirt back.

Sample	Location of Sample*	Fabric Weight (g)	Fabric Volume (cm ³)	Mass BP-3 Extracted (µg)	BP-3 Concentration in Sample (µg/cm ³)
Clean fabric	n/a	0.170	0.603	0	0
Shirt worn by subject 1	UR	0.167	0.593	22.9	38.6
	LR	0.186	0.661	24.4	37.0
	LL	0.166	0.587	23.2	40.1
	UL	0.213	0.754	30.2	38.8
Shirt worn by subject 2	UR	0.161	0.571	16.9	29.6
	LR	0.157	0.557	11.3	20.2
	LL	0.208	0.736	21.1	28.6
	UL	0.181	0.643	10.9	17.0
Shirt worn by subject 3	UR	0.199	0.706	18.2	25.8
	LR	0.181	0.643	10.9	16.9
	LL	0.187	0.663	12.4	18.6
	UL	0.160	0.569	18.4	32.3
Unworn shirt	UR	0.227	0.806	16.4	20.4
	LR	0.202	0.717	12.6	17.5
	LL	0.289	1.025	19.8	19.3
	UL	0.206	0.730	10.9	14.9
				Overall Mean	26.2
				Std. Dev.	8.92

The results show average BP-3 concentrations per shirt ranging from 17.0 to 40.1 µg/cm³. Figure 4.1: BP-3 Concentration in DTU Samples shows the average concentration of BP-3 in each shirt. The standard deviation is used to represent the error bars (1.4, 6.2, 7.1, and 2.4, respectively).

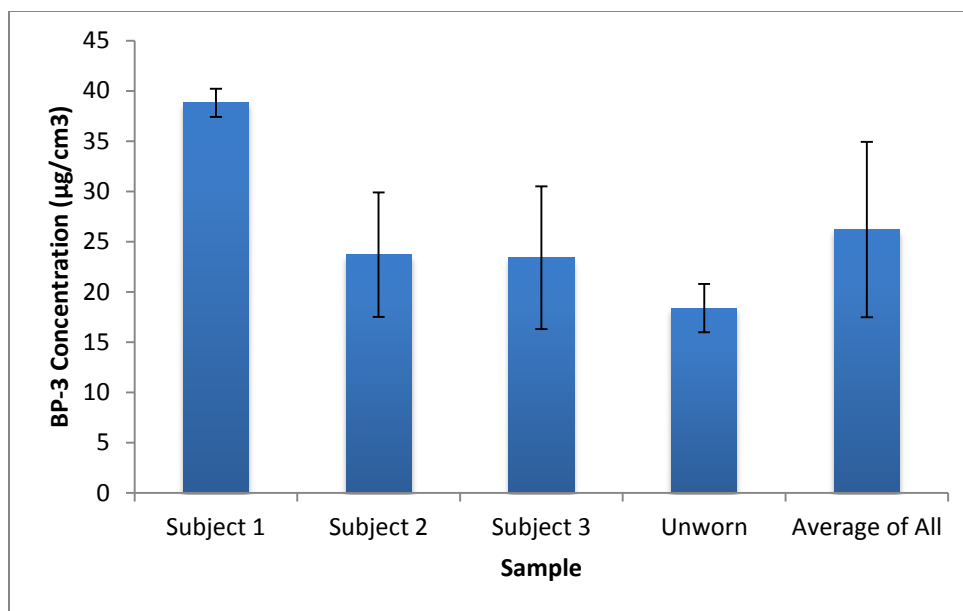


Figure 4.1: BP-3 Concentration in DTU Samples

The range of concentrations is suspected to be due to the manner by which the shirts were exposed in the dosing chamber at DTU. Before the human exposure experiment, the shirts were hung in a small chamber above three aluminum pans coated with BP-3. A small fan was placed near the pans and pointed at the shirts during the 32-day equilibration period. It is important to note that the shirt worn by subject 1 was closest to the fan and blocked the flow of air to the other shirts. The concentration of BP-3 is lower in the other shirts, which results in the likelihood that all shirts were not at equilibrium. The shirt worn by subject 1, which was closest to the fan, had the lowest standard deviation ($1.3 \mu\text{g}/\text{cm}^3$) between the four samples taken from it. This supports the idea that shirt 1 was closest to equilibrium. It should be noted that participants would likely have varying degrees of moisture on their skin, skin permeability, and skin area in direct contact with the shirts. These factors could play a large role in dermal transfer and

skin absorption, which could have caused the large range of concentrations between the shirts.

4.1.4. Partition Coefficient for BP-3 from DTU Experiment. $K_{\text{cloth-air}}$ was calculated for each fabric sample using the analytical method described in 3.4.10. The results can be seen in Table 4.3: Cloth-Air Partition Coefficient of BP-3 at 25 °C and Figure 4.2: $K_{\text{cloth-air}}$ from DTU experiment. The standard deviation was used to represent the error bars in Figure 4.2.

Table 4.3: Cloth-Air Partition Coefficient of BP-3 at 25 °C

Sample		$K_{\text{cloth-air}}$	Log10 $K_{\text{cloth-air}}$
Shirt1	Mean	8.82×10^6	6.95
	St. Dev.	3.11×10^5	5.49
Shirt 2	Mean	5.42×10^6	6.73
	St. Dev.	1.41×10^6	6.15
Shirt 3	Mean	5.32×10^6	6.73
	St. Dev.	1.61×10^6	6.21
Unworn Shirt	Mean	4.10×10^6	6.53
	St. Dev.	5.4×10^5	5.73
Overall	Mean	6.77×10^6	6.75
	St. Dev.	2.1×10^6	6.32

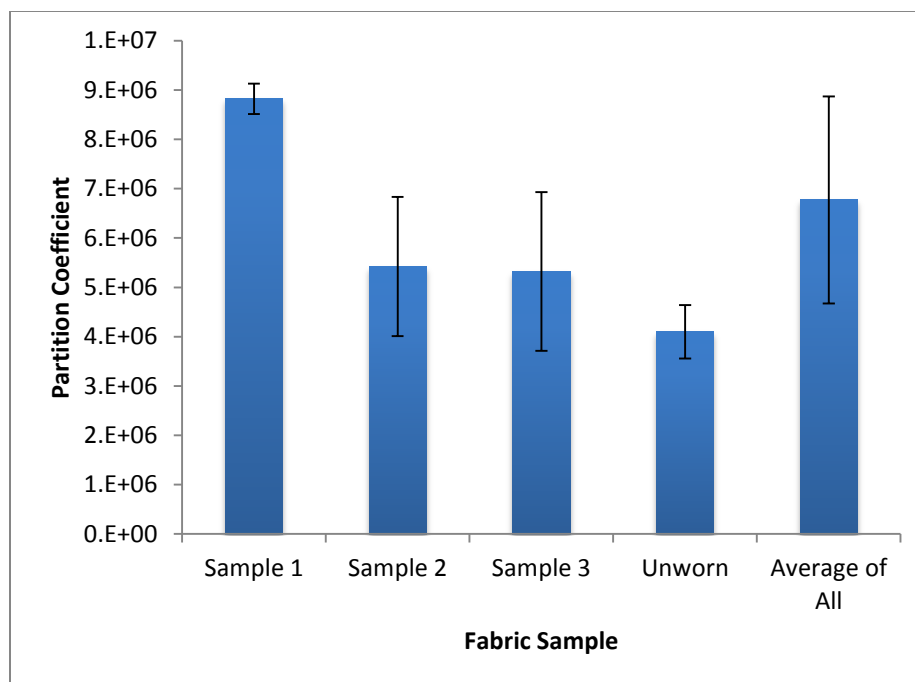


Figure 4.2: $K_{\text{cloth-air}}$ from DTU Experiment

The partition coefficients ranged from 3.93×10^6 to 8.46×10^6 . The overall average partition coefficient was 5.91×10^6 ($-\log_{10} K_{\text{cloth-air}} = 6.77$) with a standard deviation of 2.10×10^5 . As previously mentioned in 4.1.3., it is believed that the shirt worn by subject 1 was the closest sample to equilibrium. If shirt 1 is closest to equilibrium, then the partition coefficient calculated for shirt 1 should be the most accurate measurement of $K_{\text{cloth-air}}$ (8.82×10^6).

4.2. PARTITION COEFFICIENT USING SPME HEADSPACE ANALYSIS

$K_{\text{cloth-air}}$ for BP-3 was also calculated using SPME headspace analysis. First, the vapor pressure of BP-3 was determined using the gas-saturation method. The vapor pressure of BP-3 was used as a correction factor for the SPME headspace analysis of BP-3. Fabric samples were then spiked with a known mass of BP-3 and the headspace air

was analyzed using SPME analysis. The partition coefficient is the ratio of the BP-3 concentration in the fabric and in the headspace air.

4.2.1. Vapor Pressure of BP-3 Using Saturation Tube. The vapor pressure of BP-3 at various temperatures was determined using the gas-saturation method described in 3.2.1 and 3.4.11. No BP-3 was detected on the breakthrough sorption tubes. The results are shown in Table 4.4: Saturation Tube Results at Various Temperatures.

Table 4.4: Saturation Tube Results at Various Temperatures

Temp (°C)	Concentration (ng/L)	Vapor Pressure (Pa)	-Log ₁₀ Vapor Pressure (Pa)	
25	23.2	2.52E-04	3.60	
	25.3	2.74E-04	3.56	
	35.7	3.87E-04	3.41	
	Mean	28.1	3.05E-04	3.52
	Std. Dev.	6.7	7.24E-05	4.14
27	44.7	4.88E-04	3.31	
	94.0	1.03E-03	2.99	
	48.9	5.35E-04	3.27	
	Mean	62.5	6.83E-04	3.17
	Std. Dev.	27.3	2.99E-04	3.52
31	117.9	1.31E-03	2.88	
	175.6	1.95E-03	2.71	
	80.3	8.89E-04	3.05	
	Mean	124.6	1.38E-03	2.86
	Std. Dev.	48.0	5.32E-04	3.27
35	331.3	3.72E-03	2.43	
	299.8	3.37E-03	2.47	
	420.6	4.72E-03	2.33	
	Mean	239.2	3.94E-03	2.41
	Std. Dev.	62.6	7.03E-04	3.15

The $-\log_{10}$ vapor pressure of BP-3 at 25, 27, 31, and 35 °C was 3.52, 3.17, 2.86, and 2.41 where the vapor pressure is in Pa units, respectively. The standard deviation was

used as to represent the error bars. Figure 4.3., BP-3 Vapor pressure vs. Temperature, shows measurements conducted in this study along with measurements made at a different range of temperatures by Lago et al. [22]. Figure 4.4: BP-3 Vapor Pressure vs. Temperature shows the same data but with $1000/T$ (K) on the x-axis and $\text{Log}_{10}(P_v)$ on the y-axis.

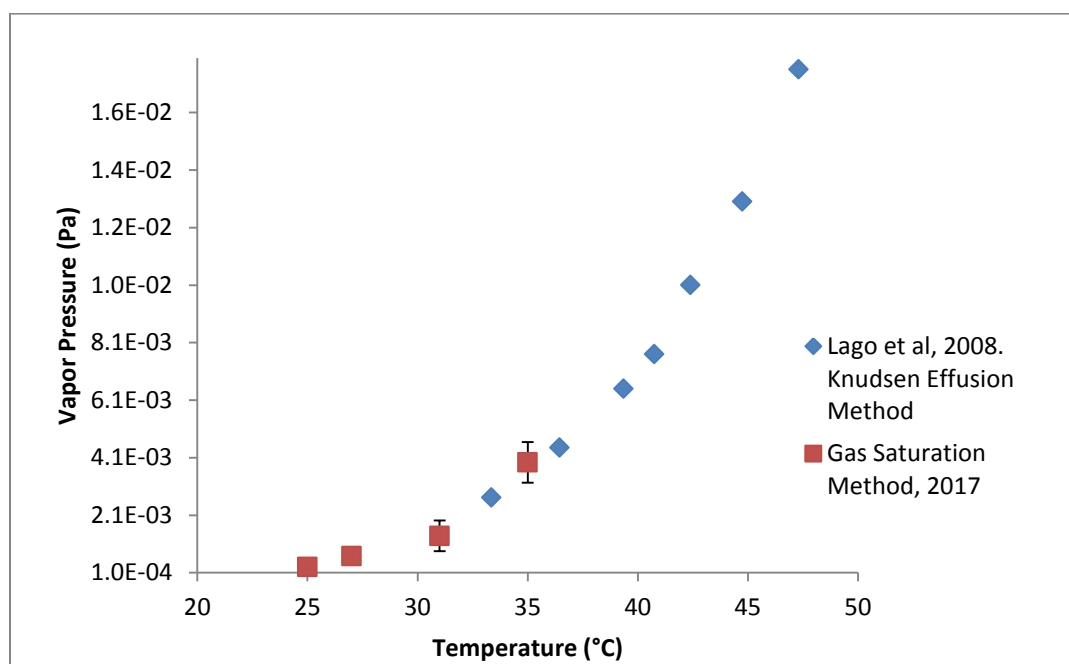


Figure 4.3: BP-3 Vapor Pressure vs. Temperature

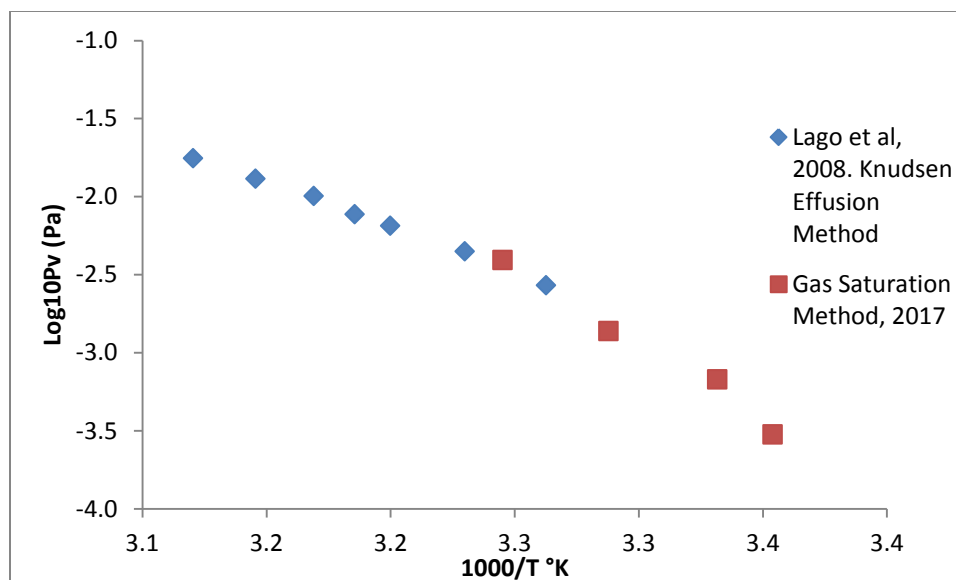


Figure 4.4: Vapor Pressure vs. Temperature

The vapor pressure of BP-3 measured using the gas-saturation method follows a trend with measurements from Lago et al. The overlap of these two sets of data gives confidence to the accuracy of the gas-saturation method measurements. However, only the data collected using the gas-saturation method was used in the correction factor for the SPME analysis, as measurements internal to this study were given preference.

4.2.2. Correction Factor for SPME Analysis. A correction factor was measured to relate the peak area from the chromatogram of the FID-GC/SPME analysis to an air concentration of BP-3. A temperature of 31 °C was chosen for the SPME analysis because it is close to the temperature of human skin at room temperature [73]. The initial measurements from the vial coated with BP-3 resulted in a correction factor of 0.627 using equation 3.4.12. After considerable use of the FID-GC, system maintenance and changes, and after the original SPME fiber breaking, the correction factor was measured again and determined to be 0.387. This correction factor of 0.387 was used for the analysis of the shirts spiked with BP-3 and for the analysis of DTU sample 1.

4.2.3. Partition Coefficient from SPME Headspace Analysis. Measurement of $k_{\text{cloth-air}}$ for BP-3 was attempted using SPME headspace analysis. The first attempt at this verification was made using fabric cut from 100% cotton denim jeans because they were readily available at the time of testing. The fabric samples were slightly larger than described in section 3.4.13. due to their estimated thickness of 1 mm. Each denim sample had a total volume of 1.44 cm^3 . The fabrics were spiked with 50, 100, and 200 μg BP-3 and were left to equilibrate at ambient temperature for one week. However, the temperature during analysis was $31 \text{ }^\circ\text{C}$ because the heat from the GC instrument warmed the sample tray. The analysis was done using $31 \text{ }^\circ\text{C}$ for the correction factor with the anticipation that the results would have some inherent inaccuracy from the unsteady temperature conditions of the vials. Using the correction factor of 0.627 as determined in section 4.2.2., the headspace air concentration was measured for each sample of cloth. $K_{\text{cloth-air}}$ was then calculated using equation 4.5. The calculated partition coefficients ranged from 2.99×10^6 to 3.41×10^6 , with an average of 3.14×10^6 . This data can be seen Table 4.5: BP-3 SPME Analysis at $31 \text{ }^\circ\text{C}$ (100% cotton denim fabric).

Table 4.5: BP-3 SPME Analysis at $31 \text{ }^\circ\text{C}$ (100% cotton denim fabric)

Mass on Fabric (μg)	Air Concentration ($\mu\text{g}/\text{m}^3$)	$K_{\text{cloth-air}}$
0	0	n/a
50	10.17	3.41×10^6
100	23.20	2.99×10^6
200	45.77	3.03×10^6
	Average	3.14×10^6
	St. Dev.	0.2×10^6

As a first attempt, these results were only used for guidance towards the next step in the study. The average partition coefficient of 3.14×10^6 is smaller than the average $k_{\text{cloth-air}}$ measured from the clothing of the DTU experiment (5.68×10^6). This smaller partition coefficient measured in denim could be because of several reasons. First, a smaller partition coefficient is expected with higher temperatures because of an increase in vapor pressure [61, 64]. Additionally, differences in fabric are now expected to play a large role in SVOC partitioning.

Next, a fabric of similar composition to the shirts worn in the DTU experiments was used (thin 100% cotton). Fabric samples were prepared as described in 3.4.13. They were allowed 24 hours to equilibrate at 31 °C. Using the correction factor of 0.387 as determined in section 4.2.2., the headspace air concentration was measured for each mass of BP-3 added to the fabric. $K_{\text{cloth-air}}$ was then calculated using equation 4.5. The calculated partition coefficients ranged from 1.2×10^7 to 1.9×10^8 , with an average of 1.1×10^8 . The results from the second SPME analysis are in Table 4.6: BP-3 SPME analysis at 31 °C (100% cotton shirt). The asterisks in Table 4.6 indicate that no response was detected for the given sample.

Table 4.6: BP-3 SPME analysis at 31 °C (100% cotton shirt)

Mass on Fabric (μg)	Air Conc. ($\mu\text{g}/\text{m}^3$)	$K_{\text{cloth-air}}$	$K_{\text{cloth-air}}$ Average
0	0	n/a	n/a
25	0.21	1.2×10^8	
25	0.33	7.7×10^7	9.9×10^7
25	0*	n/a	
50	0.26	1.9×10^8	
50	0*	n/a	1.2×10^8
50	1.10	4.6×10^7	
100	1.30	7.7×10^7	
100	1.47	6.8×10^7	6.5×10^7
100	2.01	5.0×10^7	
		Total Avg.	9.0×10^7
		St. Dev.	5.1×10^7

The fact that two of the results had no BP-3 response is troubling. This poses the possibility that the SPME extraction time is insufficient, or that the dosing procedure should be carefully examined. There could also be a leak in the headspace vial, or the concentration could be very close to the limit of detection. Perhaps using substantially longer extraction times would give more reliable peaks for integration, but a relationship between peak area and extraction time would first need to be established. The partition coefficients reported for the highest mass spiked on fabric (100 μg BP-3) are probably the most reliable because of the strong signal reported by the FID-GC/SPME.

Lastly, the shirt worn by subject 1 was prepared for headspace analysis. This shirt was chosen because of the low standard deviation of BP-3 concentrations throughout various locations in the shirt. Three fabric samples sized 4 cm x 12 cm were cut from the shirt, placed and sealed in headspace vials, and then left to equilibrate at 31 °C in the temperature controlled box. Using the correction factor of 0.387 as determined in section

4.2.2., the headspace air concentration was measured for each mass of BP-3 added to the fabric. $K_{\text{cloth-air}}$ was then calculated using equation 4.5. The average BP-3 concentration of $36.8 \mu\text{g}/\text{cm}^3$ as determined in section 4.1.3 was used for the $K_{\text{cloth-air}}$ calculation. The calculated partition coefficients ranged from 1.05×10^7 to 2.07×10^7 , with an average of 1.66×10^7 . The results from the third SPME analysis are in Table 4.7: Headspace analysis of clothing worn by subject 1 from DTU experiment (31 °C).

Table 4.7: Headspace analysis of Sample 1 from DTU experiment (31 °C)

Sample	BP-3 Concentration ($\mu\text{g}/\text{cm}^3$)	Air Conc. ($\mu\text{g}/\text{m}^3$)	$K_{\text{cloth-air}}$
1	36.8	2.88	2.07×10^7
2	36.8	5.68	1.05×10^7
3	36.8	3.20	1.86×10^7
		Mean	1.66×10^7
		Std. Dev.	5.39×10^6

4.3. COMPARISON OF $K_{\text{CLOTH-AIR}}$ MEASUREMENTS

The partition coefficients calculated in this study were measured at 25 and 31 °C. The data from the extractions at 25 °C will aid in refining the clothing-dosing protocol for future human exposure experiments. But more importantly, the data at 31 °C adds to the dermal uptake models, as 31 °C represents the temperature of human skin and the air temperature adjacent to the contaminated clothing. No direct comparison can be made between $K_{\text{cloth-air}}$ measured from the extractions and the headspace analysis because of the difference in temperature. The partition coefficients from both methods are shown in Figure 4.5 Partition Coefficients from both methods, with standard deviations representing the error bars.

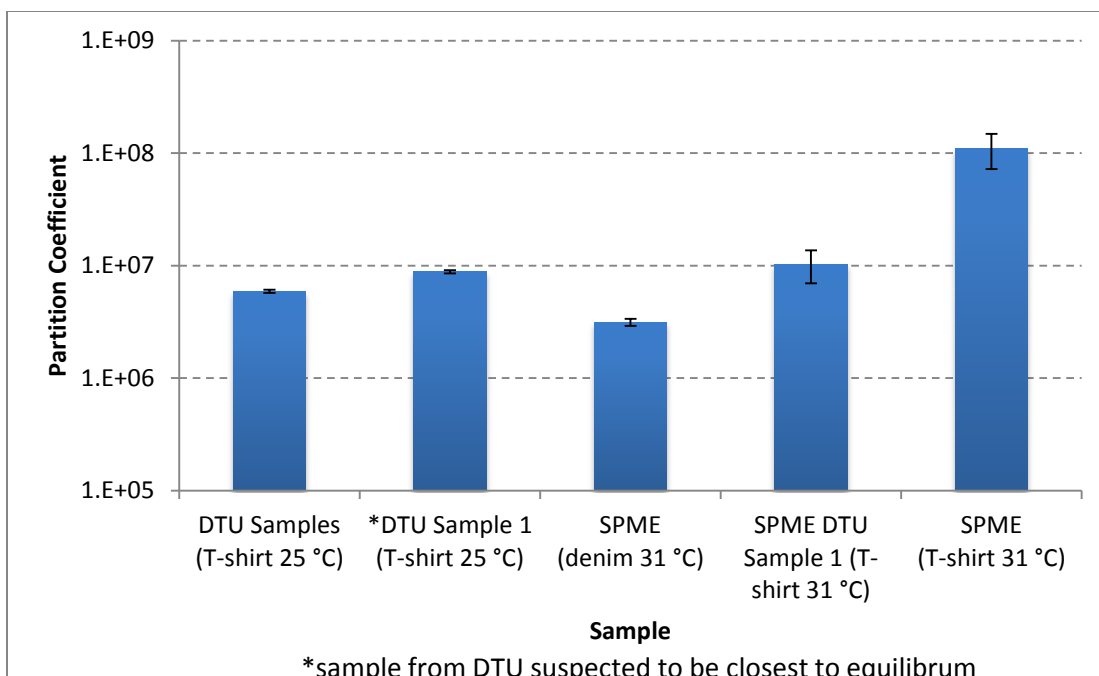


Figure 4.5: Partition Coefficients from both methods

One striking result is the large difference between the two fabrics analyzed using the SPME method (denim and T-shirt). Fabric type and temperature were the only two variables that changed between these measurements. The denim samples equilibrated at ambient temperature (approx. 22 °C), and were analyzed while sitting in a sample holder at 31 °C. Because the samples were not equilibrated at 31 °C, it is a safe assumption that the air temperature in the vials at the time of analysis was less than 31 °C. However, if temperature was the only variable, then the partition coefficient should be higher for the samples at the lower temperature. Because this is not the case, the type of fabric is the only remaining variable that could have affected the results. Fabrics of the same material likely undergo different production methods, and could have highly variable partition coefficients with SVOCs in air. Fabrics are sized with various types of water soluble polymers such as starch, polyvinyl alcohols, and acrylates in order to add some stiffness

to the material during the manufacturing process [74]. It is possible that BP-3 has a higher affinity towards the compound used for textile sizing in denim jeans than in cotton. An investigation into the types of sizing compounds used in different fabrics would help further understand this interaction.

It is also interesting that when analyzed using the SPME method at 31 °C, $K_{\text{cloth-air}}$ for sample 1 from DTU and the similar T-shirt material varied by over an order of magnitude (1×10^7 vs 1.1×10^8 , respectively). Given that the temperatures were the same and the mass of BP-3 on the shirts was comparable, the large difference in $K_{\text{cloth-air}}$ is likely due to different manufacturing methods and shirt-sizing compounds.

There could also be additional compartments within the vial that BP-3 is equilibrating with, such as the inner glass walls and the PTFE liner on the inside of the lid. Kim et al. noted sorptive losses for SVOCs to glass during their experiments to determine Henry's law constants [75]. They concluded that gas-tight syringes were unfit for their purposes due to high sorptive losses of SVOCs to glass. This should not pose a problem if enough time is given for equilibration, but could potentially be an issue if the BP-3 is still equilibrating with the compartments of the vial.

Due to the large difference in measured partition coefficients, further sampling and method improvements are necessary. However, due to the frequent use of the FID-GS/SPME by multiple research groups, instrumental downtime for maintenance, and the even more frequent use of the Peak temperature control boxes, further sampling could not be done within the time constraints of this study. Fortunately for the justification of the SPME headspace analysis, method improvements have been the focus of extensive research for one Ph.D. student in this research group.

5. CONCLUSIONS

This study did not fully complete all of its objectives. The concentration of BP-3 in the shirts from the DTU experiment was successfully quantified. The partition coefficient of BP-3 at the conditions of the DTU experiment was calculated. Verification of this partition coefficient using SPME headspace analysis was attempted, but the results show that improvements in the headspace method are needed.

5.1. OBJECTIVE 1.

The first objective was to quantify the concentration of BP-3 in the shirts from the DTU experiment.

5.1.1. Objective 1 Conclusion. This study successfully quantified the concentration of BP-3 in the shirts using solvent extraction and HPLC analysis. The result of the extractions also served to provide the researchers conducting the DTU experiments with valuable information regarding their clothing preparation techniques and aided in the interpretation of their results.

5.1.2. Objective 1 Suggestions for the Future. The methods used to achieve the first objective of this study gave satisfactory results and will likely be used for further SVOC extractions from cloth. Further recovery experiments will need to be performed for other SVOCs and fabrics of interest.

5.2. OBJECTIVE 2.

The second objective was to calculate the effective partition coefficient of BP-3 in cloth and air.

5.2.1. Objective 2 Conclusions. The second objective was successfully completed by comparing the results of the BP-3 extractions and the BP-3 air concentration data from the DTU experiment.

5.2.2. Objective 2 Suggestions for the Future. The method for achieving objective 2 is reliable and will be used for further partition coefficient investigations. While the effective $K_{\text{cloth-air}}$ was successfully calculated, the accuracy of the final result is still uncertain. The clothing under investigation was initially worn in human exposure experiments, and the quantification of $k_{\text{cloth-air}}$ was a secondary objective of a larger study. One major improvement would be to dose of pieces of clothing that are not intended to be worn, as direct dermal transfer from worn clothing would decrease the concentration of BP-3 in the fabric. Because the BP-3 concentration in the shirts was varied, it can be assumed that the shirts were not at equilibrium with the chamber air. Clothing to be worn in future experiments should be exposed in the chamber for long enough to come to equilibrium. To improve this process fans should be set at the source of BP-3 or other SVOC emission and aimed at all clothing evenly, pieces of clothing should be spaced adequately, and the source of BP-3 or other SVOC emission should be as large as possible. The partition coefficients calculated in this study could also be used to estimate the time required to reach equilibrium. Although this study determined $K_{\text{cloth-air}}$, the method improvements would be beneficial for future human exposure experiments as well.

5.3. OBJECTIVE 3.

The third objective was to use SPME headspace analysis to measure the partition coefficient of oxybenzone in cloth and air.

5.3.1. Objective 3 Conclusions. The third objective was partially completed. A method was developed to determine $K_{\text{cloth-air}}$ using SPME headspace analysis, but improvements are warranted.

5.3.2. Objective 3 Suggestions for the Future. There are several improvements that could be made on the methods used for Objective 3:

- One improvement would be to use a large fabric sample in the headspace vial to achieve the highest possible surface area of cloth. It is suspected that surface area plays a significant role in equilibration, but the data presented here doesn't adequately demonstrate this. Further investigation on the impact of fabric surface area on equilibration time should be made to address this concern.
- It is possible that the procedure for spiking fabrics with BP-3 or other SVOCs might not be 100% effective. Some of the solute may bleed through the fabric and be left behind on the Teflon sheet during the spiking procedure. Performing an extraction BP-3 from the spiked fabrics to insure that 100% of the mass of solute is absorbed by the fabric is worth investigating.
- Lastly, the materials used in the preparation of textiles should also be investigated, as the interaction of SVOCs with various textile sizing chemicals are expected to play a role in cloth-air partitioning of SVOCs.

After addressing the shortcomings of the headspace analysis, the method should be employed to verify the partition coefficient of BP-3 in cloth and air for the DTU samples at 25 °C.

REFERENCES

1. Bekö, G., et al., *Children's Phthalate Intakes and Resultant Cumulative Exposures Estimated from Urine Compared with Estimates from Dust Ingestion, Inhalation and Dermal Absorption in Their Homes and Daycare Centers*. PLoS ONE, 2013. 8(4).
2. Little, J.C., et al., *Rapid methods to estimate potential exposure to semivolatile organic compounds in the indoor environment*. Environmental Science and Technology, 2012. 46(20): p. 11171-11178.
3. Weschler, C.J. and W.W. Nazaroff, *SVOC exposure indoors: Fresh look at dermal pathways*. Indoor Air, 2012. 22(5): p. 356-377.
4. Weschler, C.J. and W.W. Nazaroff, *Semivolatile organic compounds in indoor environments*. Atmospheric Environment, 2008. 42(40): p. 9018-9040.
5. Weschler, C.J. and W.W. Nazaroff, *Dermal uptake of organic vapors commonly found in indoor air*. Environmental Science and Technology, 2014. 48(2): p. 1230-1237.
6. Xu, Y. and J. Zhang, *Understanding SVOCs*. ASHRAE Journal, 2011. 53(12): p. 121-125.
7. Balmer, M.E., et al., *Occurrence of some organic UV filters in wastewater, in surface waters, and in fish from Swiss lakes*. Environmental Science and Technology, 2005. 39(4): p. 953-962.
8. Brausch, J.M. and G.M. Rand, *A review of personal care products in the aquatic environment: Environmental concentrations and toxicity*. Chemosphere, 2011. 82(11): p. 1518-1532.
9. Calafat, A.M., et al., *Exposure to bisphenol A and other phenols in neonatal intensive care unit premature infants*. Environmental Health Perspectives, 2009. 117(4): p. 639-644.
10. Calafat, A.M., et al., *Concentrations of the sunscreen agent benzophenone-3 in residents of the United States: National Health and Nutrition Examination Survey 2003-2004*. Environmental Health Perspectives, 2008. 116(7): p. 893-897.
11. Kim, S. and K. Choi, *Occurrences, toxicities, and ecological risks of benzophenone-3, a common component of organic sunscreen products: A mini-review*. Environment International, 2014. 70: p. 143-157.
12. Zenker, A., H. Schmutz, and K. Fent, *Simultaneous trace determination of nine organic UV-absorbing compounds (UV filters) in environmental samples*. Journal of Chromatography A, 2008. 1202(1): p. 64-74.

13. Kawamura, Y., et al., *Estrogenic activities of UV stabilizers used in food contact plastics and benzophenone derivatives tested by the yeast two-hybrid assay*. Journal of Health Science, 2003. 49(3): p. 205-212.
14. Wan, Y., J. Xue, and K. Kannan, *Occurrence of benzophenone-3 in indoor air from Albany, New York, USA, and its implications for inhalation exposure*. Science of the Total Environment, 2015. 537: p. 304-308.
15. Benning, J.L., et al., *Characterizing gas-particle interactions of phthalate plasticizer emitted from vinyl flooring*. Environmental Science and Technology, 2013. 47(6): p. 2696-2703.
16. He, J. and R. Balasubramanian, *A study of gas/particle partitioning of SVOCs in the tropical atmosphere of Southeast Asia*. Atmospheric Environment, 2009. 43(29): p. 4375-4383.
17. Kanazawa, A., et al., *Association between indoor exposure to semi-volatile organic compounds and building-related symptoms among the occupants of residential dwellings*. Indoor Air, 2010. 20(1): p. 72-84.
18. Morrison, G., N.V. Shakila, and K. Parker, *Accumulation of gas-phase methamphetamine on clothing, toy fabrics, and skin oil*. Indoor Air, 2015. 25(4): p. 405-414.
19. Wu, C.C., et al., *Dermal Uptake from Airborne Organics as an Important Route of Human Exposure to E-Waste Combustion Fumes*. Environmental Science and Technology, 2016. 50(13): p. 6599-6605.
20. Morrison, G.C., et al., *Role of clothing in both accelerating and impeding dermal absorption of airborne SVOCs*. Journal of Exposure Science and Environmental Epidemiology, 2016. 26(1): p. 113-118.
21. Morrison, G.C., et al., *Dermal uptake of benzophenone-3 from clothing (article in preparation)*. 2017.
22. Lago, A.F., et al., *Thermochemistry and Gas-Phase Ion Energetics of 2-Hydroxy-4-methoxy-benzophenone (Oxybenzone)*. The Journal of Physical Chemistry A, 2008. 112(14): p. 3201-3208.
23. Jansen, R., et al., *Photoprotection: Part II. Sunscreen: Development, efficacy, and controversies*. Journal of the American Academy of Dermatology, 2013. 69(6): p. 867.e1-867.e14.
24. Wensing, M., E. Uhde, and T. Salthammer, *Plastics additives in the indoor environment - Flame retardants and plasticizers*. Science of the Total Environment, 2005. 339(1-3): p. 19-40.

25. Weschler, C.J., T. Salthammer, and H. Fromme, *Partitioning of phthalates among the gas phase, airborne particles and settled dust in indoor environments*. Atmospheric Environment, 2008. 42(7): p. 1449-1460.
26. Yang, Y., et al., *Determination of phthalate plasticizers in daily foods and their migration from food packages*. Se pu = Chinese journal of chromatography / Zhongguo hua xue hui, 2013. 31(7): p. 674-678.
27. Morrison, G., et al., *Airborne phthalate partitioning to cotton clothing*. Atmospheric Environment, 2015. 115: p. 149-152.
28. Wang, L., et al., *Indoor SVOC pollution in China: A review*. Chinese Science Bulletin, 2010. 55(15): p. 1469-1478.
29. Ait Bamai, Y., et al., *Associations of phthalate concentrations in floor dust and multi-surface dust with the interior materials in Japanese dwellings*. Science of the Total Environment, 2014. 468-469: p. 147-157.
30. Blanchard, O., et al., *Semivolatile organic compounds in indoor air and settled dust in 30 French dwellings*. Environmental Science and Technology, 2014. 48(7): p. 3959-3969.
31. Centers for Disease Control., *Fourth National Report on Human Exposure to Environmental Chemicals*. Alternative Medicine Review, 2010.15(2):101-109.
32. Cohen Hubal, E.A., et al., *Measuring potential dermal transfer of a pesticide to children in a child care center*. Environmental Health Perspectives, 2006. 114(2): p. 264-269.
33. Fenske, R.A., et al., *Potential exposure and health risks of infants following indoor residential pesticide applications*. American Journal of Public Health, 1990. 80(6): p. 689-693.
34. Guo, Y. and K. Kannan, *Comparative assessment of human exposure to phthalate esters from house dust in China and the United States*. Environmental Science and Technology, 2011. 45(8): p. 3788-3794.
35. Gurunathan, S., et al., *Accumulation of chlorpyrifos on residential surfaces and toys accessible to children*. Environmental Health Perspectives, 1998. 106(1): p. 9-16.
36. Liroy, P.J., *Assessing total human exposure to contaminants. A multidisciplinary approach*. Environmental Science & Technology, 1990. 24(7): p. 938-945.
37. Weschler, C.J., et al., *Transdermal uptake of diethyl phthalate and di(n-butyl) phthalate directly from air: Experimental verification*. Environmental Health Perspectives, 2015. 123(10): p. 928-934.

38. Morrison, G.C., C.J. Weschler, and G. Bekö, *Dermal uptake directly from air under transient conditions: advances in modeling and comparisons with experimental results for human subjects*. *Indoor Air*, 2016. 26(6): p. 913-924.
39. Bekö, G., et al., *Measurements of dermal uptake of nicotine directly from air and clothing*. *Indoor Air*, 2016. 27: p. 427-433.
40. Lautenschlager, S., H.C. Wulf, and M.R. Pittelkow, *Photoprotection*. *The Lancet*. 370(9586): p. 528-537.
41. Janjua, N.R., et al., *Systemic absorption of the sunscreens benzophenone-3, octyl-methoxycinnamate, and 3-(4-methyl-benzylidene) camphor after whole-body topical application and reproductive hormone levels in humans*. *Journal of Investigative Dermatology*, 2004. 123(1): p. 57-61.
42. Schlumpf, M., et al., *Exposure patterns of UV filters, fragrances, parabens, phthalates, organochlor pesticides, PBDEs, and PCBs in human milk: Correlation of UV filters with use of cosmetics*. *Chemosphere*, 2010. 81(10): p. 1171-1183.
43. Fent, K., A. Zenker, and M. Rapp, *Widespread occurrence of estrogenic UV-filters in aquatic ecosystems in Switzerland*. *Environmental Pollution*, 2010. 158(5): p. 1817-1824.
44. Kameda, Y., K. Kimura, and M. Miyazaki, *Occurrence and profiles of organic sun-blocking agents in surface waters and sediments in Japanese rivers and lakes*. *Environmental Pollution*, 2011. 159(6): p. 1570-1576.
45. Philippat, C., et al., *Prenatal exposure to environmental phenols: Concentrations in amniotic fluid and variability in urinary concentrations during pregnancy*. *Environmental Health Perspectives*, 2013. 121(10): p. 1225-1231.
46. Tsui, M.M.P., et al., *Occurrence, distribution and ecological risk assessment of multiple classes of UV filters in surface waters from different countries*. *Water Research*, 2014. 67: p. 55-65.
47. Cuderman, P. and E. Heath, *Determination of UV filters and antimicrobial agents in environmental water samples*. *Analytical and Bioanalytical Chemistry*, 2007. 387(4): p. 1343-1350.
48. Negreira, N., et al., *Sensitive determination of salicylate and benzophenone type UV filters in water samples using solid-phase microextraction, derivatization and gas chromatography tandem mass spectrometry*. *Analytica Chimica Acta*, 2009. 638(1): p. 36-44.

49. Loraine, G.A. and M.E. Pettigrove, *Seasonal variations in concentrations of pharmaceuticals and personal care products in drinking water and reclaimed wastewater in Southern California*. Environmental Science and Technology, 2006. 40(3): p. 687-695.
50. Schlumpf, M., et al., *In vitro and in vivo estrogenicity of UV screens*. Environmental Health Perspectives, 2001. 109(3): p. 239-244.
51. Schlecht, C., et al., *Effects of estradiol, benzophenone-2 and benzophenone-3 on the expression pattern of the estrogen receptors (ER) alpha and beta, the estrogen receptor-related receptor 1 (ERR1) and the aryl hydrocarbon receptor (AhR) in adult ovariectomized rats*. Toxicology, 2004. 205(1-2): p. 123-130.
52. Schmutzler, C., et al., *Endocrine disruptors and the thyroid gland-a combined in vitro and in vivo analysis of potential new biomarkers*. Environmental Health Perspectives, 2007. 115(SUPPL1): p. 77-83.
53. French, J.E., *NTP technical report on the toxicity studies of 2-Hydroxy-4-methoxybenzophenone (CAS No. 131-57-7) Administered Topically and in Dosed Feed to F344/N Rats and B6C3F1 Mice*. Toxic Rep Ser, 1992. 21: p. 1-E14.
54. Blüthgen, N., S. Zucchi, and K. Fent, *Effects of the UV filter benzophenone-3 (oxybenzone) at low concentrations in zebrafish (Danio rerio)*. Toxicology and Applied Pharmacology, 2012. 263(2): p. 184-194.
55. Kinnberg, K.L., et al., *Endocrine-disrupting effect of the ultraviolet filter benzophenone-3 in zebrafish, Danio rerio*. Environmental Toxicology and Chemistry, 2015. 34(12): p. 2833-2840.
56. Danovaro, R., et al., *Sunscreens cause coral bleaching by promoting viral infections*. Environmental Health Perspectives, 2008. 116(4): p. 441-447.
57. Downs, C.A., et al., *Toxicopathological Effects of the Sunscreen UV Filter, Oxybenzone (Benzophenone-3), on Coral Planulae and Cultured Primary Cells and Its Environmental Contamination in Hawaii and the U.S. Virgin Islands*. Archives of Environmental Contamination and Toxicology, 2016. 70(2): p. 265-288.
58. Leo, A., C. Hansch, and D. Elkins, *Partition coefficients and their uses*. Chemical Reviews, 1971. 71(6): p. 525-616.
59. Staudinger, J. and P.V. Roberts, *A critical review of Henry's law constants for environmental applications*. Critical Reviews in Environmental Science and Technology, 1996. 26(3): p. 205-297.
60. Mackay, D.S., W., *A critical review of Henry's law constants for environmental applications*. Journal of Physical and Chemical Reference Data, 1981. 10(4): p. 205-297.

61. Saini, A., et al., *From air to clothing: Characterizing the accumulation of semi-volatile organic compounds to fabrics in indoor environments*. *Indoor Air*, 2016. 26: p.1-11.
62. Tolls, J., *Sorption of veterinary pharmaceuticals in soils: A review*. *Environmental Science and Technology*, 2001. 35(17): p. 3397-3406.
63. Weschler, C.J. and W.W. Nazaroff, *SVOC partitioning between the gas phase and settled dust indoors*. *Atmospheric Environment*, 2010. 44(30): p. 3609-3620.
64. Saini, A., et al., *Characterizing the sorption of polybrominated diphenyl ethers (PBDEs) to cotton and polyester fabrics under controlled conditions*. *Science of the Total Environment*, 2016. 563-564: p. 99-107.
65. Westcott, J.W., C.G. Simon, and T.F. Bidleman, *Determination of polychlorinated biphenyl vapor pressures by a semimicro gas saturation method*. *Environmental Science & Technology*, 1981. 15(11): p. 1375-1378.
66. *Standard Test Method for Thickness of Textile Materials*. 2015, ASTM International. D1777-96, 2011.
67. Bhuva, C.S., R.; Sharma, A., *Analytical Method Development For Simultaneous Estimation Of Oxybenzone, Octocrylene, Octinoxate And Avobenzone In Sunscreen By High Performance Liquid Chromatography And Its Validation*. *Pharmacophore*, 2012. 3(2).
68. Kasichayanula, S., et al., *Simultaneous analysis of insect repellent DEET, sunscreen oxybenzone and five relevant metabolites by reversed-phase HPLC with UV detection: Application to an in vivo study in a piglet model*. *Journal of Chromatography B: Analytical Technologies in the Biomedical and Life Sciences*, 2005. 822(1-2): p. 271-277.
69. Buechlein, M., *Particle mediated enhanced mass transfer of diethylhexyl phthalate: A pilot scale system design*. *Scholars' Mine*, 2016. 7498.
70. van der Veen, I., et al., *Development and validation of a method for the quantification of extractable perfluoroalkyl acids (PFAAs) and perfluorooctane sulfonamide (FOSA) in textiles*. *Talanta*, 2016. 147: p. 8-15.
71. Luongo, G., et al., *Determination of aniline and quinoline compounds in textiles*. *Journal of Chromatography A*, 2016. 1471: p. 11-18.
72. Luongo, G., G. Thorsén, and C. Östman, *Quinolines in clothing textiles—a source of human exposure and wastewater pollution?* *Analytical and Bioanalytical Chemistry*, 2014. 406(12): p. 2747-2756.
73. Olesen, B.W. and P.O. Fanger, *The skin temperature distribution for resting man in comfort*. *ARCH.SCI.PHYSIOL.*, 1973. 27(4): p. 385-393.

74. Meshram, M.W., et al., *Graft copolymers of starch and its application in textiles*. Carbohydrate Polymers, 2009. 75(1): p. 71-78.
75. Kim, Y.-H. and K.-H. Kim, *Test on the Reliability of Gastight Syringes as Transfer/Storage Media for Gaseous VOC Analysis: The Extent of VOC Sorption between the Inner Needle and a Glass Wall Surface*. Analytical Chemistry, 2015. 87(5): p. 3056-3063.

VITA

Jon Hill was born in Independence, Missouri. In May 2015, he received his B.S. with Honors in Environmental Science from Lincoln University in Jefferson City, Missouri. In May 2017, he received his M.S. in Environmental Engineering from the Missouri University of Science and Technology. Jon has participated in research symposiums and coauthored journal papers. Jon was awarded the Chancellor's Fellowship in August 2016 to fund his M.S. in Environmental Engineering.